Journal of Pharmaceutical Analysis 13 (2023) 1562–1576

Contents lists available at ScienceDirect

Journal of Pharmaceutical Analysis

journal homepage: www.elsevier.com/locate/jpa

Original article

Integrating UHPLC-MS/MS quantitative analysis and exogenous purine supplementation to elucidate the antidepressant mechanism of Chaigui granules by regulating purine metabolism

Jiajun Chen [a, b, c, 1], Tian Li [a, b, c, 1], Dehua Huang [a, b, c], Wenxia Gong [a, b, c], Junsheng Tian [a, b, c], Xiaoxia Gao [a, b, c], Xuemei Qin [a, b, c], Guanhua Du [a, d], Yuzhi Zhou [a, b, c, *]

[a] Modern Research Center for Traditional Chinese Medicine, Shanxi University, Taiyuan, 030006, China
[b] The Key Laboratory of Chemical Biology and Molecular Engineering of Ministry of Education, Shanxi University, Taiyuan, 030006, China
[c] The Key Laboratory of Effective Substances Research and Utilization in TCM of Shanxi Province, Taiyuan, 030006, China
[d] Institute of Materia Medica, Chinese Academy of Medical Sciences & Peking Union Medical College, Beijing, 100050, China

ARTICLE INFO

Article history:
Received 28 March 2023
Received in revised form
14 July 2023
Accepted 10 August 2023
Available online 17 August 2023

Keywords:
Chaigui granules
Traditional Chinese medicine
Antidepressant mechanism
Purine metabolism
Purinergic signaling

ABSTRACT

Chaigui granules (CG) are a compound composed of six herbal medicines with significant antidepressant effects. However, the antidepressant mechanism of CG remains unclear. In the present study, we attempted to elucidate the antidepressant mechanism of CG by regulating purine metabolism and purinergic signaling. First, the regulatory effect of CG on purine metabolites in the prefrontal cortex (PFC) of chronic unpredictable mild stress (CUMS) rats was analyzed by ultra high-performance liquid chromatography tandem mass spectrometry (UHPLC-MS/MS) targeted quantitative analysis. Meanwhile, purinergic receptors (P2X7 receptor (P2X7R), A_1 receptor (A_1R) and A_{2A} receptor (A_{2A}R)) and signaling pathways (nod-like receptor protein 3 (NLRP3) inflammasome pathway and cyclic adenosine monophosphate (cAMP)-protein kinase A (PKA) pathway) associated with purine metabolism were analyzed by western blotting and enzyme-linked immunosorbent assay (ELISA). Besides, antidepressant mechanism of CG by modulating purine metabolites to activate purinergic receptors and related signaling pathways was dissected by exogenous supplementation of purine metabolites and antagonism of purinergic receptors in vitro. An in vivo study showed that the decrease in xanthine and the increase in four purine nucleosides were closely related to the antidepressant effects of CG. Additionally, purinergic receptors (P2X7R, A_1R and A_{2A}R) and related signaling pathways (NLRP3 inflammasome pathway and cAMP-PKA pathway) were also significantly regulated by CG. The results of exogenous supplementation of purine metabolites and antagonism of purinergic receptors showed that excessive accumulation of xanthine led to activation of the P2X7R-NLRP3 inflammasome pathway, and the reduction of adenosine and inosine inhibited the A_1R-cAMP-PKA pathway, which was significantly ameliorated by CG. Overall, CG could promote neuroprotection and ultimately play an antidepressant role by inhibiting the xanthine-P2X7R-NLRP3 inflammasome pathway and activating the adenosine/inosine-A_1R-cAMP-PKA pathway.

© 2023 The Authors. Published by Elsevier B.V. on behalf of Xi'an Jiaotong University. This is an open access article under the CC BY-NC-ND license (http://creativecommons.org/licenses/by-nc-nd/4.0/).

1. Introduction

Depression is the leading cause of mental health disease burden, as well as the major cause of disability worldwide, severely affecting social life [1]. Meanwhile, existing treatments for depression are dominated by antidepressant drugs, which cause some side effects and often require months to achieve effect [2]. Thus, safe and effective antidepressant drugs are urgently needed. Although depression is accompanied by metabolic disorders such as glutamate metabolism, energy metabolism and purine metabolism [3–5], there are limited biomarkers in these metabolic pathways that could be used as clinical diagnostics for depression and have not been fully explored. Moreover, the biological mechanisms underlying the regulation of depression by key metabolites in these metabolic pathways have not been fully elucidated, making it difficult to concatenate the core logic of biological regulation, which not only reduces the reliability of biomarker screening, but

Peer review under responsibility of Xi'an Jiaotong University.
* Corresponding author. Modern Research Center for Traditional Chinese Medicine, Shanxi University, Taiyuan, 030006, China.
E-mail address: zhouyuzhi@sxu.edu.cn (Y. Zhou).
[1] Both authors equally contributed to this work.

https://doi.org/10.1016/j.jpha.2023.08.008
2095-1779/© 2023 The Authors. Published by Elsevier B.V. on behalf of Xi'an Jiaotong University. This is an open access article under the CC BY-NC-ND license (http://creativecommons.org/licenses/by-nc-nd/4.0/).

also overlooks potential novel targets for depression regulation. Currently, investigating the modulatory effects of antidepressant drugs on the metabolome, thereby identifying functional metabolites and further dissecting the deep biological significance, will facilitate the screening of clinical diagnostic biomarkers and the development of new antidepressant drugs.

With the escalating demand for new antidepressant medicines, traditional Chinese medicine (TCM) has received increasing attention due to its unique efficacy in depression treatment [6]. Chaigui granules (CG) are an emerging antidepressant herbal compound (clinical approval number: 2018L03149, Chinese National Medical Products Administration) developed from the classic antidepressant herbal prescription Xiaoyao San (XYS), which consists of six Chinese herbs (*Bupleurum chinense*, *Angelica sinensis*, *Radix Paeoniae Alba*, *Atractylodes macrocephala*, *Glycyrrhiza uralensis* and *Mentha haplocalyx*). In past studies, CG have shown significant antidepressant effects with unique natural advantages in terms of safety and efficacy [7,8], but the antidepressant mechanism of CG remains unclear. Notably, our previous study revealed that the antidepressant effect of CG was related to the regulation of purine metabolism in peripheral blood mononuclear cells (PBMCs) of chronic unpredictable mild stress (CUMS) rats [7], whereas the regulatory effect of CG on purine metabolism in the brain was unknown and required further investigation.

As early as 1972, the purinergic signaling hypothesis was proposed by Geoffrey Burnstock [9] and was applied to explore the pathogenesis of neuropsychiatric diseases, such as depression [10]. After long-term research, it has been found that purine metabolites (such as purine nucleosides) could act on purinergic receptors to participate in neuromodulation [11,12]. Recently, a growing amount of clinical and preclinical evidence has suggested that disordered purine metabolism is associated with the pathogenesis of depression [13,14]. However, a large number of studies have only shown the phenomenon of purine metabolism disorder in the pathogenesis of depression, whereas the mechanism of depression induced by dysregulated purine metabolism has not been fully clarified. In terms of purinergic receptors, purinergic P2X7 receptor (P2X7R), A_1 receptor (A_1R) and A_{2A} receptor (A_{2A}R) have been considered to be involved in the occurrence and development of depression [15–17], and P2X7R antagonists have been applied in the development of antidepressant drugs [18–20]. However, the relationship between purine metabolites and purinergic receptors is still unclear. Therefore, it is of great significance to screen purine metabolites that regulate these purinergic receptors. Additionally, the cyclic adenosine monophosphate (cAMP)-protein kinase A (PKA) pathway and the nod-like receptor protein 3 (NLRP3) inflammasome pathway have been reported as potential pathways for purinergic receptors to regulate depression [21,22], broadly involved in neuromodulation [23,24], whereas the relationship between purinergic receptors and related signaling pathways needs further study. Overall, previous studies have suggested that the purine metabolite-purinergic receptor-purinergic signaling pathway axis plays a significant role in the regulation of depression, which might represent a novel way to treat depression by regulating purine metabolism.

The prefrontal cortex (PFC) acts as the chief executive officer of the brain, controlling the highest level of cognitive and emotional processes [25] and playing a crucial role in the pathogenesis of depression [26]. In this study, purine metabolites in the PFC were quantitatively determined by ultra high-performance liquid chromatography tandem mass spectrometry (UHPLC-MS/MS) based on multiple reaction monitoring (MRM) mode, and the changes in purinergic receptors and related signaling pathways were characterized by western blotting and enzyme-linked immunosorbent assay (ELISA) to explore the regulatory effect of CG on purine metabolism and purinergic signaling. Additionally, the process of purinergic signaling transmission and the regulation of CG were analyzed by corticosterone (CORT)-injured PC12 cell depression model, and the purinergic signaling axis was dissected by integrating exogenous supplementation of purine metabolites and biological antagonism. Ultimately, taking the above results together, the antidepressant mechanism of CG based on the regulation of purine metabolism and purinergic signaling in the brain was elucidated (Fig. 1). Predominantly, the current research dissected the antidepressant mechanism of CG from the perspective of purinergic signaling, and provided a novel insight into the pathogenesis of depression and the development of antidepressant drugs.

2. Materials and methods

2.1. Chemicals and reagents

Purine standards of adenosine-5′-monophosphate (AMP), inosine-5′-monophosphate (IMP), guanosine-5′-monophosphate (GMP), adenosine, inosine, xanthosine, guanosine, adenine, hypoxanthine, xanthine and guanine were purchased from Topscience (Shanghai, China). The standard 2-chlorophenylalanine was purchased from Acmec (Shanghai, China), and the standard galanthamine was purchased from Topscience (Shanghai, China). Mass spectrometry-grade acetonitrile, formic acid and methanol were purchased from Thermo Fisher Scientific (Waltham, MA, USA). Phosphate buffered saline (PBS) and nonfat powdered milk were purchased from Sangon (Shanghai, China). Bovine serum albumin (BSA) and Tris-base were purchased from Solarbio (Beijing, China). Glycine was purchased from Macklin (Shanghai, China). Primary antibodies against A_1R (anti-ADORA1), A_{2A}R (anti-ADORA2a), P2X7R (anti-P2RX7), NLRP3 (anti-NLRP3), apoptosis-associated speck-like protein containing a CARD (ASC) (anti-ASC), caspase-1 (anti-caspase-1), PKA (anti-PKA alpha + beta) and β-actin (anti-β-actin) were purchased from Bioss (Beijing, China). Horseradish peroxidase (HRP)-conjugated secondary antibody, rhodamine B isothiocyanate (RBITC)-conjugated secondary antibody and fluorescein isothiocyanate (FITC)-conjugated secondary antibody were purchased from Bioss (Beijing, China). Roswell Park Memorial Institute (RPMI) 1640 medium, antibiotics (penicillin and streptomycin) and trypsin were purchased from Sangon (Shanghai, China). Poly-L-lysine (PLL), 3-(4,5-dimethylthiazol-2-yl)-2,5-diphenyltetrazolium bromide (MTT), dimethyl sulfoxide (DMSO) and Hoechst 33342 were purchased from Solarbio (Beijing, China). Fetal bovine serum was purchased from Every Green (Hangzhou, China). CORT was purchased from TCI (Shanghai, China). Antagonists of A_1R (DPCPX), A_{2A}R (SCH58261) and P2X7R (JNJ-47965567) were purchased from Topscience (Shanghai, China). XYS was gifted from Dr. Chen (21.78% yield, Shanxi University), and the quality control of XYS has been presented in a previous report [27]. Venlafaxine was obtained from Wyeth (Madison, NJ, USA). The item numbers and origins of the chemicals and reagents mentioned above are shown in Table S1.

2.2. Preparation of CG

Bupleurum chinense (No. 1805215131), *Angelica sinensis* (No. 1803583111), *Radix Paeoniae Alba* (No. 1806436111), *Atractylodes macrocephala* (No. 1809657151), *Glycyrrhiza uralensis* (No. 1810013171), and *Mentha haplocalyx* (No. 1802017131) were obtained from Shanxi Huayang Pharmaceutical Co., Ltd. (Taiyuan, China), and authenticated by Professor Xuemei Qin in the Pharmacognosy Department of Shanxi University. CG were entrusted to the Preparation Center of Shanxi Academy of Traditional Chinese Medicine for processing and preparation (Batch number: 20181009, 10 g/pack, containing 27.5 g crude drug).

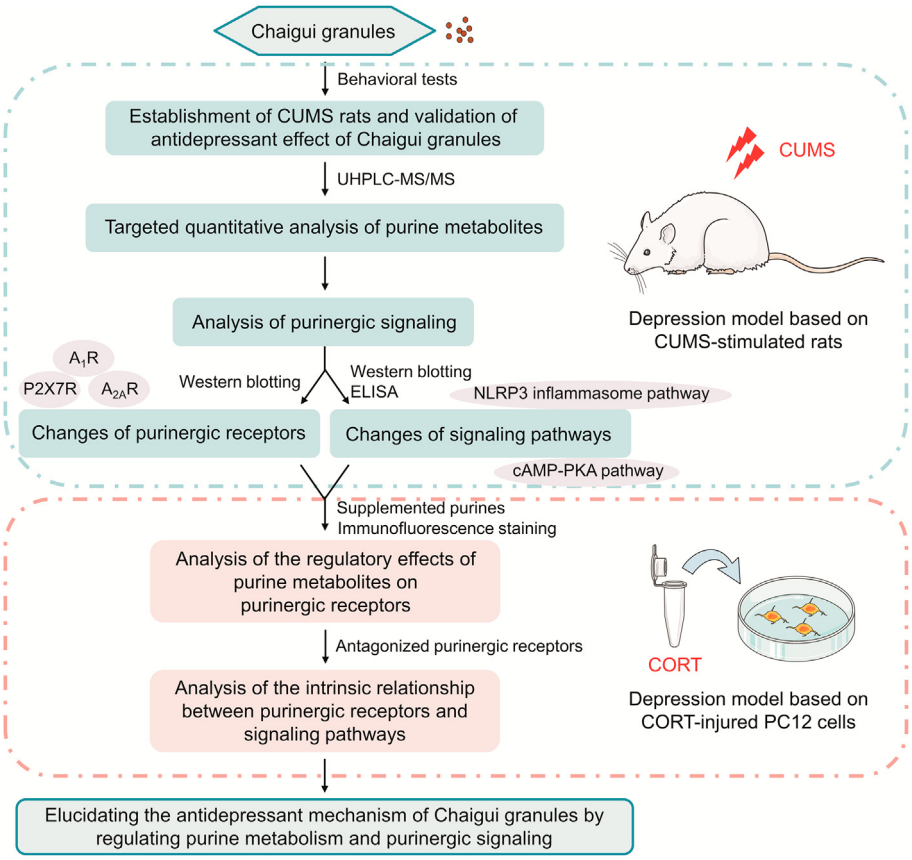

Fig. 1. Protocol for clarifying the antidepressant mechanism of Chaigui granules by modulating purine metabolism and purinergic signaling. A_1R: A_1 receptor; $A_{2A}R$: A_{2A} receptor; cAMP: cyclic adenosine monophosphate; CORT: corticosterone; CUMS: chronic unpredictable mild stress; ELISA: enzyme-linked immunosorbent assay; NLRP3: Nod-like receptor protein 3; PKA: protein kinase A; P2X7R: P2X7 receptor; UHPLC-MS/MS: ultra high-performance liquid chromatography tandem mass spectrometry.

To ensure the quality of CG, the chemical markers (saikosaponin a, saikosaponin b2 and paeoniflorin) used for quality monitoring were analyzed on an Agilent 1260 series high-performance liquid chromatography (HPLC) system (Agilent Technologies, Santa Clara, CA, USA). Chromatographic separation was performed on Agela Plus C_{18} column (250 mm × 4.6 mm, 5 μm; Agela Technologies, Tianjin, China) at 30 °C (Fig. S1). The results of chromatographic analysis indicated that the quality of CG met the requirements, and the content is provided in Tables S2 and S3.

2.3. Animals and administration

All animal studies were conducted under the NIH Guidelines for Care and Use of Laboratory Animals (USA) and the Prevention of Cruelty to Animals Act (1986) of China. This study was also approved by the Animal Ethics Committee of Shanxi University (Approval number: SXULL2020028). All male Sprague-Dawley rats (180–220 g) were acquired from Beijing Vital River Laboratory Animal Technology Co., Ltd (Certificate No. SCXK (Jing) 2016-0006; Beijing, China). Additionally, a total of 44 rats were housed in a standard environment (temperature: 20–25 °C, relative humidity: 40%–60%) with a 12 h light/12 h dark cycle, and they had free access to standard food and filtered water. After a week of adaptation, all rats were randomly grouped according to the initial behavioral results to ensure that there was no self-difference between the rats in each group. The experimental rats were divided into four groups: control group ($n = 12$), CUMS group ($n = 12$), CUMS + CG group (8.3 g crude drug/kg, $n = 12$) and CUMS + XYS group (23 g crude drug/kg, $n = 8$). The drug was administered by oral gavage daily for 28 days, and the control group and CUMS group were given 10 mL/kg of distilled water by oral gavage. In the current study, the CUMS procedure was performed as described previously [28].

2.4. Behavior tests

After 28 days of CUMS and CG administration, body weight, the sucrose preference test (SPT), open-field test (OFT), forced swimming test (FST), and elevated plus maze test (EPM) were used to assess depressive-like behavior in rats. The evaluation process of body weight, the SPT, OFT and FST was consistent with our previous report [28], and the EPM referred to a past study [29].

2.5. UHPLC-MS/MS analysis of purine metabolites

2.5.1. Preparation of standard solution

Given their low solubility, purine standards were dissolved individually in 0.01 mol/L NaOH solution. Subsequently, different volumes of standard solutions were mixed and diluted with acetonitrile to prepare stock solutions of mixed standards. The internal standard (IS) solution was produced by mixing IS1 (2-chlorophenylalanine) and IS2 (galanthamine) with acetonitrile (final concentration: IS1-1.2 μg/mL, IS2-0.15 μg/mL). The stock solution concentration of each standard is presented in Table S4.

2.5.2. Preparation of PFC samples

PFC was prepared (20 mg), acetonitrile-water (3:1, *V/V*, 400 μL) was used to precipitate proteins, and consistent IS1 and IS2 were added to each sample. After being thoroughly ground, the

suspension was centrifuged (4 °C, 12,000 rpm, 10 min) to obtain the supernatant. The resulting supernatant was dried under a gentle stream of nitrogen at room temperature and rehydrated with acetonitrile-water (1:1, *V/V*, 300 μL). Additionally, the thawed samples were centrifuged (4 °C, 12,000 rpm, 10 min), and the supernatant was aspirated. Finally, the resulting supernatant was filtered through the membrane and stored at −80 °C for later use.

2.5.3. Targeted quantitative analysis of purine metabolites

Chromatographic separation was performed using an ExionLC ultra high-performance liquid chromatography (UHPLC) system (AB SCIEX, Framingham, MA, USA) with an ACQUITY UPLC HSS T3 column (2.1 mm × 100 mm, 1.8 μm; Waters, Milford, NA, USA). Formic acid in water (0.1%) (*V/V*; solvent A) and acetonitrile (solvent B) were used as mobile phases. The gradient elution of the mobile phase was programmed as follows: 0–2 min, 0% B; 2–5 min, 0–1% B; 5–6 min, 1–3% B; 6–6.5 min, 3–10% B; 6.5–8 min, 10–20% B; 8–9 min, 20–35% B; 9–11 min, 35–95% B; 11–12 min, 95% B; 12–14 min, 95–0% B; 14–16 min, 0% B. Additionally, the flow rate of the mobile phase was 0.2 mL/min, the injected volume was 5 μL and the column was kept at 40 °C. Mass spectrometry was performed on an AB SCIEX API 3200MD equipped with a stream electrospray ionization (ESI) source (AB SCIEX, Framingham, MA, USA), and the samples were analyzed in MRM mode under positive ionization mode. The parameter information was as follows: ion source temperature, 500 °C; gas flow rate, 12 L/min; capillary voltage, 5500 V; curtain gas, 35 psi; nebulizer, 50 psi; nitrogen gas, 50 psi.

2.5.4. Methodological investigation

The ion pairs (Q1 and Q3), collision energy (CE), declustering potential (DP), and the corresponding liquid phase method and mass spectrometry method were optimized with reference to a previous report [30]. Then, the optimized method was used to investigate the specificity, linearity, precision, stability, matrix effect, extraction recovery, and dilution effect (Supplementary data). The corresponding purine metabolite concentrations of the four mixed quality control (QC) samples (QC1, QC2, QC3 and lower limit of quantitation (LLOQ, the lowest concentration of the standard curves, more than 10 times signal-to-noise ratio)) are shown in Table S5. After the UHPLC-MS/MS method was confirmed to be reliable, it was used for subsequent determination of PFC purine metabolites in rats.

2.6. Cell culture and administration

Poorly differentiated PC12 cells (Cell Bank of Chinese Academy of Sciences, China, passages 8–12) were inoculated in culture flasks with RPMI 1640 medium containing 10% fetal bovine serum and 1% antibiotics (37 °C, 95% humidity, 5% CO_2). When the PC12 cell state reached the optimum, PC12 cells were seeded on PLL (0.01%)-coated 96-well plates at 3×10^4 per/well, 6-well plates at 3×10^5 per/well, and 100 mm dishes at 2×10^6 per/dish and cultured with serum-free basal RPMI 1640 medium. After the PC12 cells were fully adhered, the supernatant was changed to drugs formulated with serum-free basal RPMI 1640 medium and cultured for 24 h.

2.7. MTT cell survival assay

After administration for 24 h, the culture medium in the 96-well plate was discarded, and MTT (0.5 mg/mL, 100 μL) prepared with basal RPMI 1640 was added to each well. After 4 h, MTT was replaced with DMSO. The microplate reader (Tecan, Männedorf, Switzerland) read the absorbance value at 570 nm wavelength.

2.8. Measurement of reactive oxygen species (ROS)

After PC12 cells in 6-well plates were treated with CORT and CG for 24 h, the 2′,7′-dichlorodihydrofluorescein diacetate (DCFH-DA) probe (Beyotime, Shanghai, China) was incubated with PC12 cells for 0.5 h to detect ROS. Additionally, Hoechst 33342 staining solution was utilized to label living cells. The distribution of ROS was observed by fluorescence microscopy (Olympus, Tokyo, Japan), and the fluorescence intensity of ROS was determined by flow cytometry (Beckman Coulter, Brea, CA, USA).

2.9. Measurement of IL-1β, IL-6, TNF-α, MDA, SOD and cAMP

Interleukin-1β (IL-1β), interleukin-6 (IL-6) and tumor necrosis factor-α (TNF-α) were measured by ELISA kits (AndyGene, Beijing, China). Malondialdehyde (MDA) and superoxide dismutase (SOD) were measured by commercial kits (Nanjing Jiancheng Technology Co., Ltd, Nanjing, China). The concentration of cAMP in the rat PFC and PC12 cells was detected by an ELISA kit (Animalunion, Shanghai, China). All steps were performed under the guidance of the instruction manual, and absorbance was read at 450 nm wavelength with a microplate reader (Tecan, Männedorf, Switzerland).

2.10. Western blot

The PFC and cell samples were lysed to acquire the protein solution. Next, the protein solution was assayed by using a bicinchoninic acid (BCA) kit (MiniBio, Shanxi, China). Western blotting was applied to determine the expression levels of P2X7R, A_1R, $A_{2A}R$, NLRP3, caspase-1, ASC and PKA. First, samples containing the same protein concentration were separated by sodium dodecyl sulfate-polyacrylamide gel electrophoresis (SDS-PAGE) gel and electrically transferred to polyvinylidene fluoride (PVDF) membranes. Subsequently, PVDF membranes were blocked with Tris-buffered saline containing 5% nonfat powdered milk. After labeling with primary (1:1,000) and secondary (HRP, 1:5,000) antibodies, the target proteins were analyzed by a ChemiDocTM XRS+ workstation (Bio-Rad, Hercules, CA, USA). The complete original images of the western blotting are shown in Figs. S2 and S3.

2.11. Immunofluorescence staining

PC12 cells (3×10^5 cells/well) were seeded into 6-well plates containing glass slides and cultured at 37 °C for 24 h. After drug treatment, 4% paraformaldehyde was utilized to fix cells. To permeabilize cells, 0.1% Triton X-100 was added later. Next, all cells were sealed with 5% BSA at 37 °C. Furthermore, P2X7R, A_1R and $A_{2A}R$ antibodies (1:200) were incubated with cells and labeled with fluorescent secondary antibodies (RBITC or FITC, 1:200). Subsequently, Hoechst 33342 solution was utilized to label the distribution of cells. Finally, each slide was sealed with glycerol, and fluorescent pictures were observed and recorded in a high-resolution live cell imaging system (GE Power, Boston, MA, USA).

2.12. Statistical analysis

Data were analyzed by SPSS 25.0 (IBM, Armonk, NY, USA), and all results are represented as the mean ± standard error of mean (SEM). Comparative analysis between multiple groups was performed by one-way analysis of variance (ANOVA) with a post hoc least significant difference (LSD) test. The following were considered to be significantly different: $^{\#}P/^{*}P/^{\&}P < 0.05$, $^{\#\#}P/^{**}P/^{\&\&}P < 0.01$, $^{\#\#\#}P/^{***}P/^{\&\&\&}P < 0.001$.

3. Results and discussion

3.1. CG treatment alleviated depressive-like behaviors in CUMS rats

To verify the antidepressant effect of CG (8.3 g crude drug/kg, dose investigation of CG was carried out in our previous work [7,8]), behavioral tests were used to evaluate the depressive-like state in rats. The schedule of administration and testing in CUMS rats is presented in Fig. 2A. As shown in the results, compared with the control group, the body weight of CUMS rats was significantly reduced, and CUMS rats exhibited obvious depressive-like behaviors in the SPT, OFT, FST and EPM (Figs. 2B–H). After four weeks of CG administration, the body weight of CUMS rats increased, and the depressive-like behaviors of CUMS rats were significantly alleviated. Notably, CG had similar antidepressant effects to XYS (Figs. 2B–E), and the antidepressant mechanism of CG was subsequently investigated.

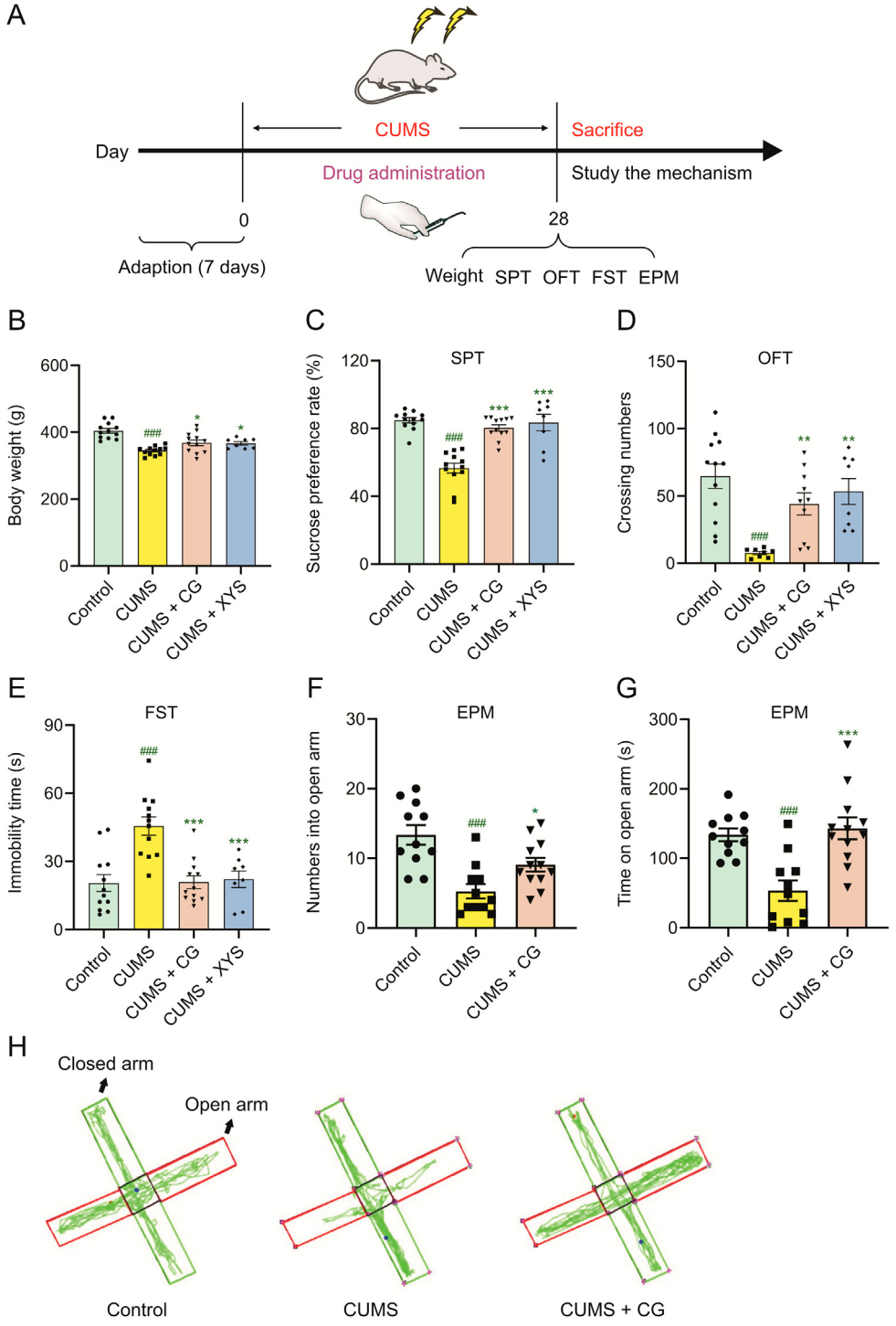

Fig. 2. Chaigui granules (CG) alleviated chronic unpredictable mild stress (CUMS)-induced depressive-like behaviors. (A) The experimental procedure design. (B) Body weight changes. (C) The sucrose preference rate of each group in the sucrose preference test (SPT). (D) Lattice crossing numbers in the open-field test (OFT). (E) Immobility time in the forced swimming test (FST). (F, G) The results of elevated plus maze test (EPM). (H) Trajectory diagrams of rats in the EPM. Data were presented as mean ± standard error of mean (SEM), $n = 12$, except for the Xiaoyao San (XYS) group ($n = 8$). $^{###}P < 0.001$, vs. control group; $^{*}P < 0.05$, $^{**}P < 0.01$, $^{***}P < 0.001$, vs. CUMS group.

3.2. Disordered purine metabolism in the PFC of CUMS rats was ameliorated by CG

Peripheral purine metabolism was identified to be associated with the antidepressant effect of CG by nontargeted metabolomics in PBMCs in our previous study [7], but the relationship between purine metabolism in the brain and the antidepressant effect of CG was unclear. Here, the levels of purine metabolites in the PFC of rats were measured by UHPLC-MS/MS.

3.2.1. Methodological investigation

As shown in Table 1, the mass spectrum information for purines is listed. After the investigation of specificity, linearity, precision, stability, matrix effect, extraction recovery and dilution effect (Figs. S4 and S5, and Tables S6–S10), the method for the detection of purine metabolites was confirmed to be accurate, stable and reliable.

3.2.2. Quantitative analysis of purine metabolites

The optimized UHPLC-MS/MS method was utilized to monitor purine metabolites in the PFC of rats from each group. Compared to the control group, adenine, hypoxanthine, guanine, adenosine, inosine, xanthosine, guanosine, AMP, IMP and GMP were significantly decreased, whereas the downstream product xanthine was significantly increased in the CUMS group, indicating that the abnormal accumulation of xanthine was closely related to the occurrence and development of depression (Fig. 3A). After CG administration, the contents of purine metabolites were significantly modulated in CUMS rats. Notably, CG exerted a stronger modulatory effect ($P < 0.001$) on purine nucleosides (adenosine, inosine, xanthosine, and guanosine) than on purine nucleotides (AMP, IMP, and GMP) and purine bases (adenine and hypoxanthine), except for reducing xanthine content (Fig. 3B). Xanthine and purine nucleosides are widely involved in neuromodulation, and consistently, our previous study also showed a significant increase in xanthine content and a significant decrease in purine nucleoside content in the brain of CUMS rats [31]. Due to the important roles of xanthine and purine nucleosides in the regulation of depression, the antidepressant mechanism of CG was dissected according to the biological functions of xanthine and four purine nucleosides (adenosine, inosine, xanthosine, and guanosine).

3.3. Purinergic receptors and related signaling pathways were regulated by CG

Given that purine metabolites can modulate depression by affecting purinergic receptors [32–34], the expression of purinergic receptors was determined by western blotting. The results showed (Fig. 4A) that the expression of P2X7R and $A_{2A}R$ was significantly increased, and the expression of A_1R was significantly decreased in the PFC of CUMS rats (Figs. 4B–D), indicating that the disturbance of purinergic receptors was involved in the development of depression. After CG administration, the abnormal expression of purinergic receptors was significantly improved. The NLRP3 inflammasome pathway and cAMP-PKA pathway could be regulated by purinergic receptors; therefore, NLRP3, caspase-1, and ASC in the NLRP3 inflammasome pathway and cAMP and PKA alpha + beta in the cAMP-PKA pathway were determined. Compared with the control group, the expression levels of NLRP3, caspase-1 and ASC were significantly increased (Figs. 4E–G), and the level of cAMP and the expression of PKA alpha + beta were significantly decreased (Figs. 4H and I) in the CUMS group, which showed that the NLRP3 inflammasome pathway was activated and the cAMP-PKA pathway was inhibited. After CG administration, the disturbance of the NLRP3 inflammasome pathway and cAMP-PKA pathway was significantly alleviated. Among them, activation of the NLRP3 inflammasome pathway was found to be associated with an increase in oxidative stress (due to excessive accumulation of xanthine) and the release of inflammatory factors in our previous study [30], and here, the regulatory effects of CG on oxidative stress and inflammatory factors were also investigated. The results showed that CUMS-induced oxidative stress and the inflammatory response could also be suppressed by CG (Figs. 4J, and S6). In this section, the antidepressant effect of CG was demonstrated to be related to the regulation of purinergic receptors and related signaling pathways.

From animal studies, purine metabolites, purinergic receptors and two purinergic signaling pathways were regulated by CG; however, it was unclear whether there were interactions between purinergic metabolites, purinergic receptors and signaling pathways, which were subsequently analyzed in a depression model of CORT-injured PC12 cells in vitro.

3.4. CG exerted antidepressant effects by reducing xanthine and increasing adenosine and inosine

In this section, the neuroprotective effects of five purine metabolites (xanthine, adenosine, inosine, xanthosine and guanosine) on CORT-injured PC12 cells were examined by exogenous supplementation of purine metabolites, and the modulatory effects of CG on these purine metabolites were determined by co-incubation of CG with purine metabolites.

Table 1
Mass spectral information for each purine metabolite in multiple reaction monitoring (MRM) mode.

Compounds	Molecular weight	Q1/Q3	CE (volts)	DP (volts)	Ion mode
Adenine	135.1	136.1–119.2	30	36	+
Hypoxanthine	136.1	137.1–110.0	20	36	+
Xanthine	152.1	153.0–110.0	15	35	+
Guanine	151.1	152.1–110.0	22	70	+
Adenosine	267.2	268.1–136.0	20	40	+
Inosine	268.2	269.1–137.1	20	21	+
Xanthosine	284.2	285.0–152.03	15	35	+
Guanosine	283.2	284.2–152.1	20	40	+
AMP	347.2	348.2–136.1	15	35	+
IMP	348.2	349.2–293.1	50	55	+
GMP	363.2	364.1–152.1	10	25	+
IS1	199.6	200.0–154.1	10	20	+
IS2	287.4	288.1–213.0	20	20	+

AMP: adenosine-5′-monophosphate; CE: collision energy; DP: declustering potential; GMP: guanosine-5′-monophosphate; IMP: inosine-5′-monophosphate; IS1: 2-chlorophenylalanine; IS2: galanthamine.

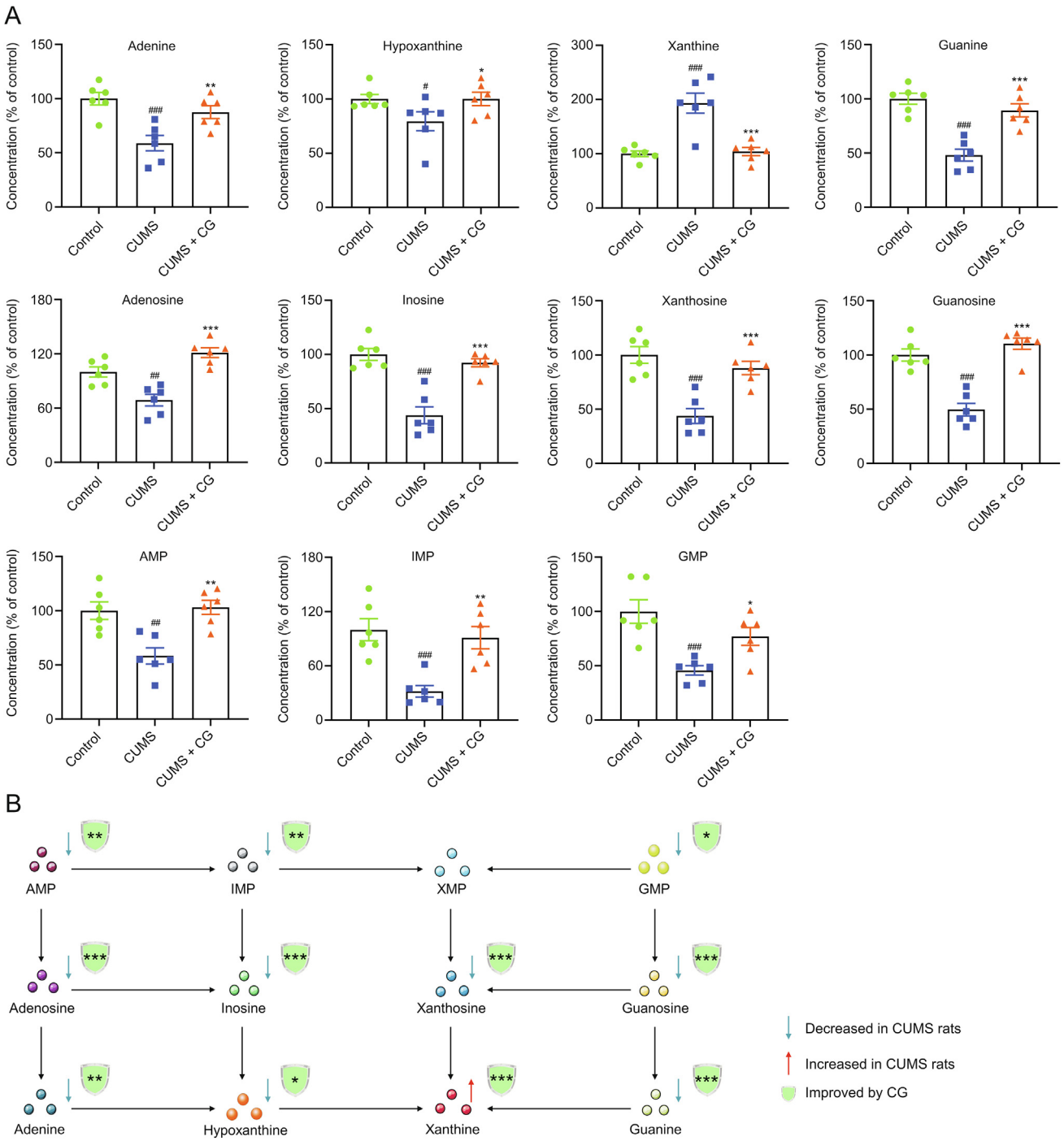

Fig. 3. Effect of Chaigui granules (CG) on purine metabolism in chronic unpredictable mild stress (CUMS)-induced depressed rats. (A) Statistical charts of targeted quantitative analysis of 11 prefrontal cortex (PFC) purine metabolites based on ultra high-performance liquid chromatography tandem mass spectrometry (UHPLC-MS/MS). (B) Schematic diagram of changes in the content of purine metabolites. Data were presented as mean ± standard error of mean (SEM), $n = 6$. $^{\#}P < 0.05$, $^{\#\#}P < 0.01$, $^{\#\#\#}P < 0.001$, vs. control group; $^{*}P < 0.05$, $^{**}P < 0.01$, $^{***}P < 0.001$, vs. CUMS group. AMP: adenosine-5′-monophosphate; GMP: guanosine-5′-monophosphate; IMP: inosine-5′-monophosphate; XMP: xanthosine-5′-monophosphate.

3.4.1. CG attenuated CORT-induced neural damage in PC12 cells

Before dissecting the specific mechanism of CG intervention in purine metabolism and purinergic signaling, a CORT-injured PC12 cell model was introduced, and the neuromodulatory effect of CG was investigated. As shown in the results, when PC12 cells were incubated with 600 μM CORT, nearly 50% of the cells were damaged (Fig. 5A). Thus, 600 μM CORT was used in subsequent cellular experiments. Next, the effects of CG (40–320 μg crude drug/mL) on PC12 cells before and after CORT injury were analyzed. The results showed that CG had no obvious effect on normal PC12 cells (Fig. 5B), but 80 and 120 μg crude drug/mL CG could significantly enhance the cell viability of CORT-injured PC12 cells (Fig. 5C), and the effect of CG was similar to that of XYS and venlafaxine (Fig. 5D). Additionally, CORT-induced ROS production was also significantly

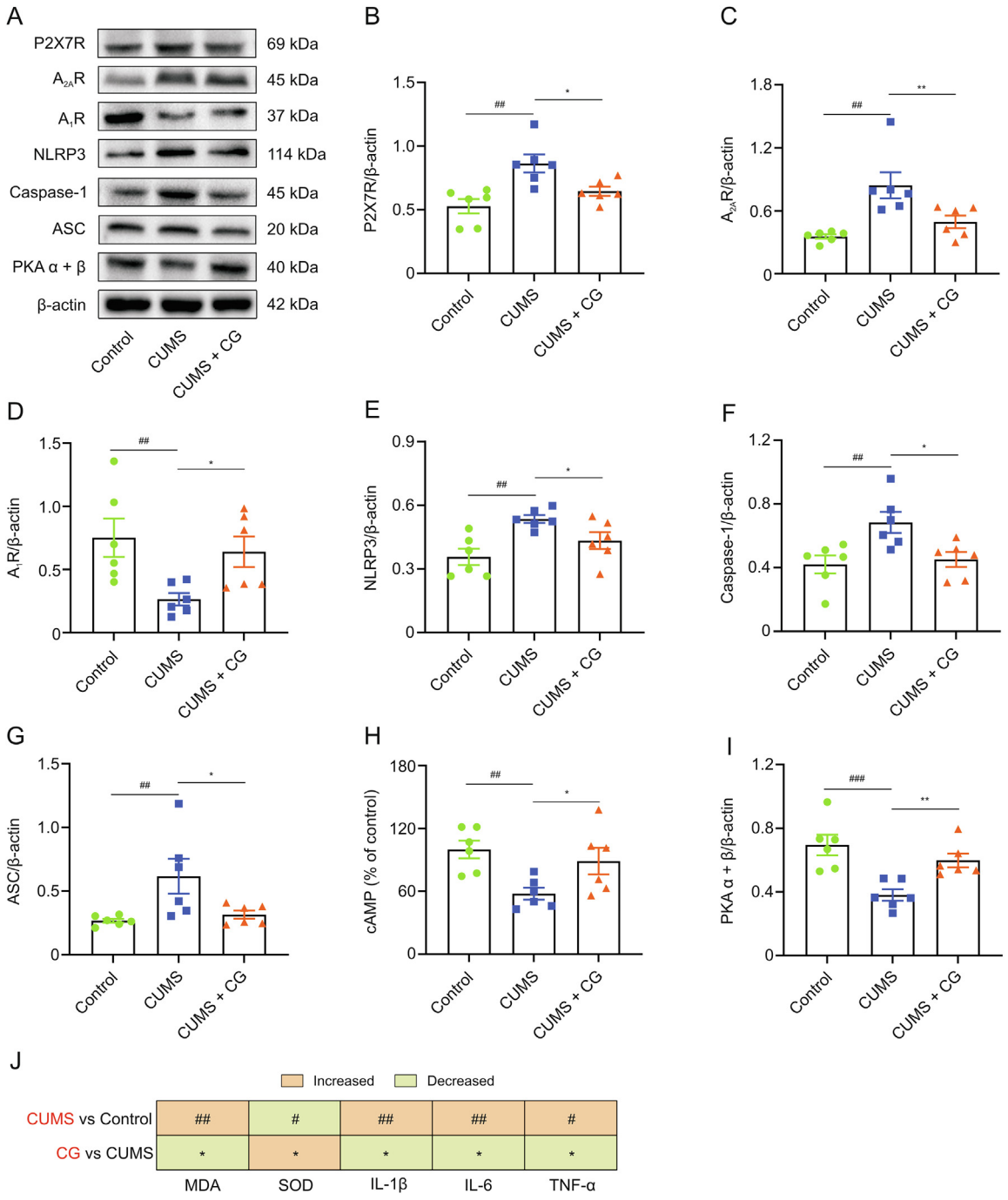

Fig. 4. Effects of Chaigui granules (CG) on purinergic receptors and related signaling pathways. (A) Western blot of purinergic receptors and purinergic signaling pathways. (B) Western blot statistics of P2X7 receptor (P2X7R). (C) Western blot statistics of A_{2A} receptor (A_{2A}R). (D) Western blot statistics of A_1 receptor (A_1R). (E) Western blot statistics of Nod-like receptor protein 3 (NLRP3). (F) Western blot statistics of caspase-1. (G) Western blot statistics of apoptosis-associated speck-like protein containing a CARD (ASC). (H) Enzyme-linked immunosorbent assay (ELISA) result for cyclic adenosine monophosphate (cAMP). (I) Western blot statistics of protein kinase A (PKA). (J) Effects of CG on malondialdehyde (MDA), superoxide dismutase (SOD), interleukin-1β (IL-1β), interleukin-6 (IL-6) and tumor necrosis factor-α (TNF-α) before and after administration. Data were presented as mean ± standard error of mean (SEM), $n = 6$. $^{\#}P < 0.05$, $^{\#\#}P < 0.01$, $^{\#\#\#}P < 0.001$, vs. control group; $^{*}P < 0.05$, $^{**}P < 0.01$, vs. chronic unpredictable mild stress (CUMS) group.

reduced by 80 and 120 μg crude drug/mL CG (Figs. 5E and F). The above results indicated that CG had a significant neuroprotective effect, and 120 μg/mL CG was used for follow-up studies.

3.4.2. CG exerted neuroprotective effects by regulating xanthine, adenosine and inosine levels

In animal studies, xanthine and four purine nucleosides were significantly regulated by CG in the PFC of CUMS rats (Fig. 3B), and we hypothesized that changes in the levels of these purine metabolites were related to the neuroprotective effects of CG. Therefore, here, exogenous supplementation of purine metabolites was employed to investigate the relationship between the five purine metabolites and neuroprotective effects. As shown in the results, xanthine and four purine nucleoside metabolites had no distinct effect on normal PC12 cells at doses of 0.005–300 μM (Fig. 6A), but had different regulatory effects on CORT-injured PC12 cells

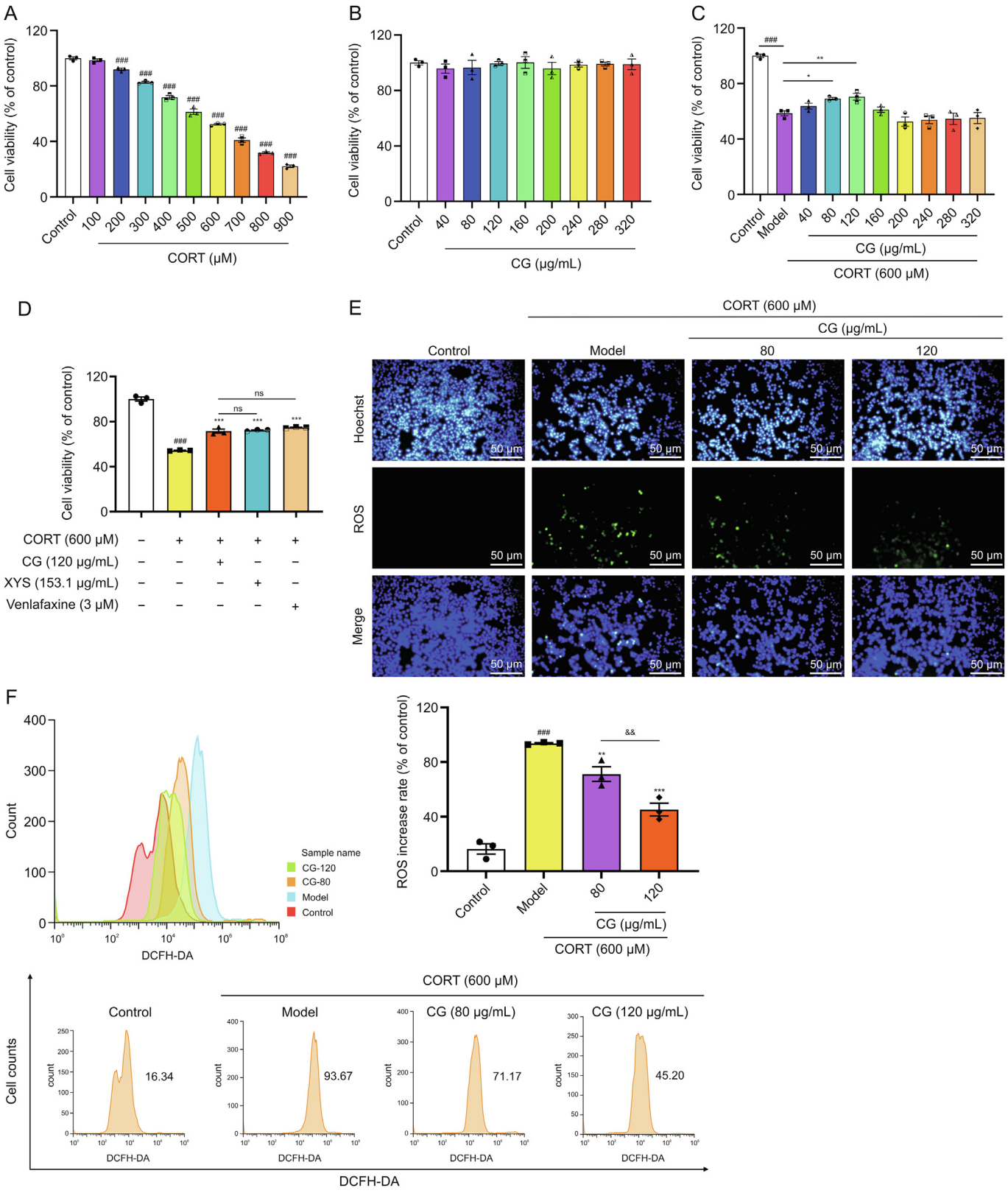

Fig. 5. Neuroprotective effect of Chaigui granules (CG) on corticosterone (CORT)-injured PC12 cells. (A) Investigation of CORT modeling dose. (B) The effect of CG on normal PC12 cells. (C) Regulation of CG on CORT-injured PC12 cells. (D) Comparison of neuroprotective effect of CG with Xiaoyao San (XYS) and venlafaxine. (E) Reactive oxygen species (ROS) fluorescence imaging. (F) ROS fluorescence intensity was measured by flow cytometry. Data were presented as mean ± standard error of mean (SEM), $n = 3$. $^{###}P < 0.001$, vs. control group; $^{*}P < 0.05$, $^{**}P < 0.01$, $^{***}P < 0.001$, vs. model group; $^{\&\&}P < 0.01$, vs. CG (120 μg/mL) group; ns: no significant difference. DCFH-DA: 2′,7′-dichlorodihydrofluorescein diacetate.

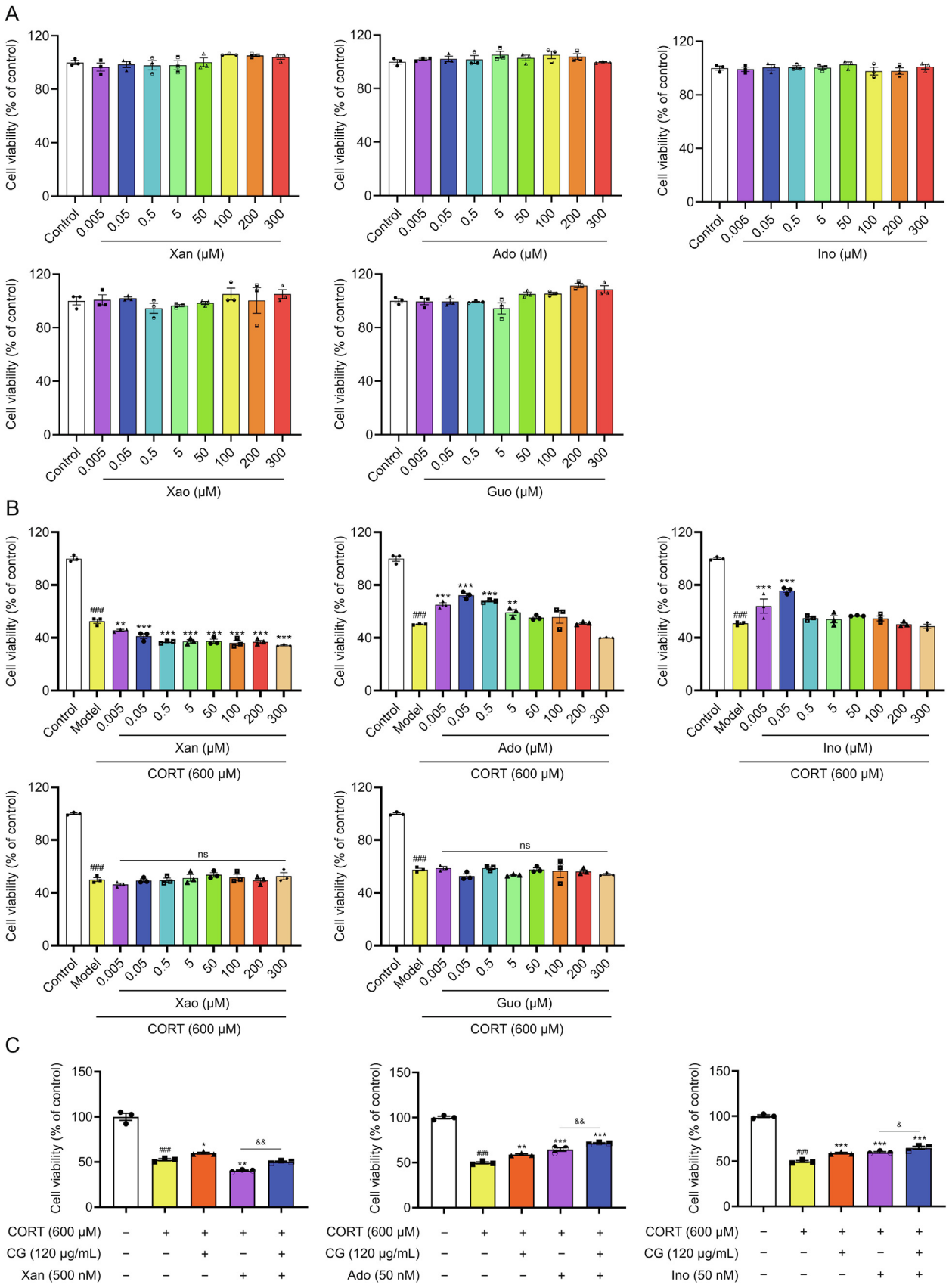

Fig. 6. Effects of Chaigui granules (CG) on the neuromodulatory functions of xanthine (Xan) and purine nucleosides. (A) Effects of Xan and purine nucleosides on normal PC12 cells. (B) Neuromodulation of Xan and purine nucleosides on corticosterone (CORT)-injured PC12 cells. (C) Effects of Xan, adenosine (Ado) and inosine (Ino) co-incubated with CG on CORT-injured PC12 cells. Data were presented as mean ± standard error of mean (SEM), $n = 3$. $^{\#\#\#}P < 0.001$, vs. control group; $^{*}P < 0.05$, $^{**}P < 0.01$, $^{***}P < 0.001$, vs. CORT group; $^{\&}P < 0.05$, $^{\&\&}P < 0.01$, vs. co-incubation group of purine metabolites and CG; ns: no significant difference. Guo: guanosine; Xao: xanthosine.

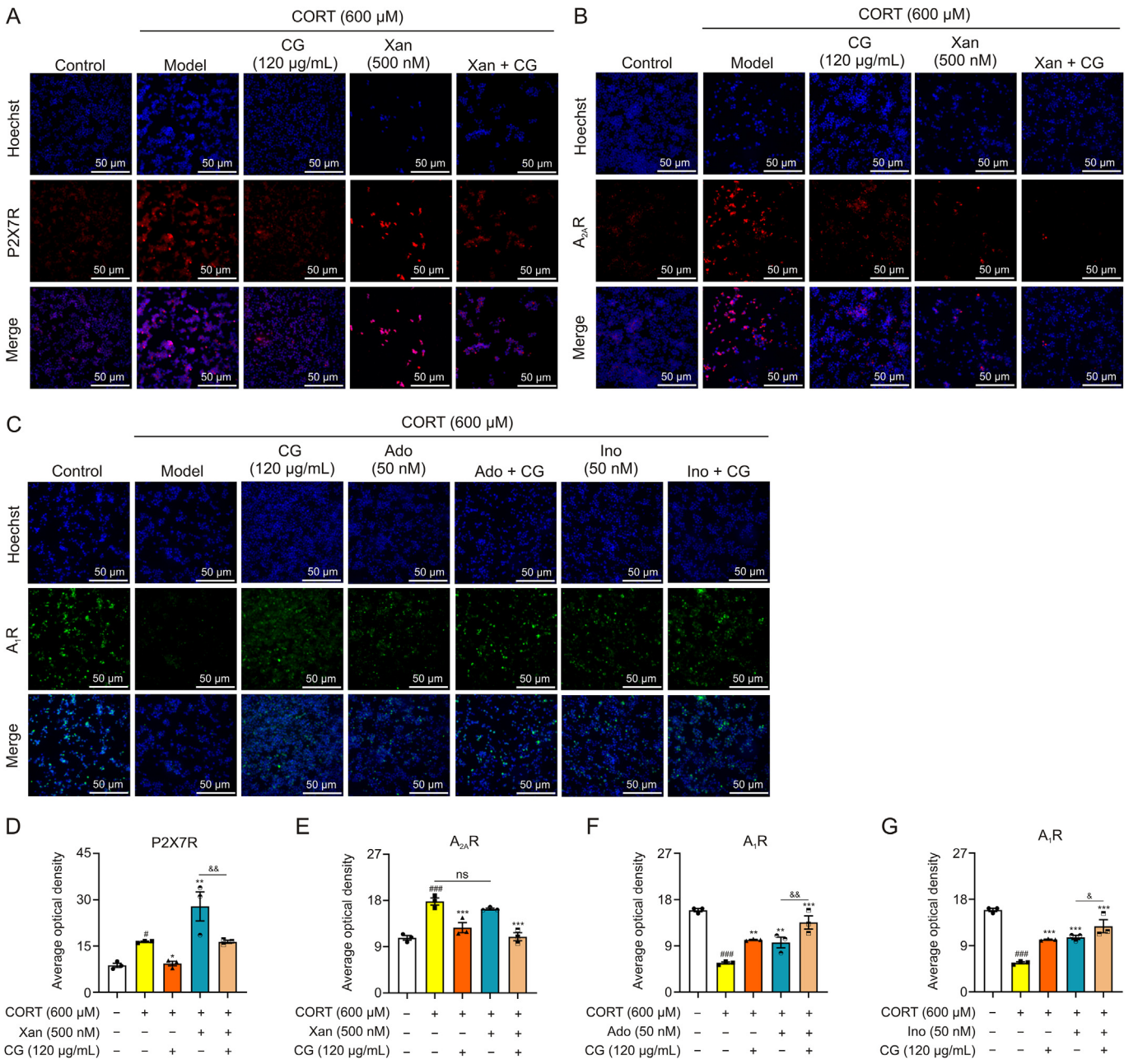

Fig. 7. Effects of exogenous supplementation of purine metabolites on purinergic receptor expression. (A) Effects of exogenous xanthine (Xan) supplementation on the expression of P2X7 receptor (P2X7R) in corticosterone (CORT)-injured PC12 cells. (B) Effects of exogenous Xan supplementation on A_{2A} receptor (A_{2A}R) expression in CORT-injured PC12 cells. (C) Effects of exogenous supplementation of adenosine (Ado) and inosine (Ino) on A_1 receptor (A_1R) expression in CORT-injured PC12 cells. (D) Statistical plot of P2X7R immunofluorescence staining. (E) Statistical plot of A_{2A}R immunofluorescence staining. (F) Statistical plot of A_1R immunofluorescence staining before and after adenosine supplementation. (G) Statistical plot of A_1R immunofluorescence staining before and after inosine supplementation. Data were presented as mean ± standard error of mean (SEM), $n = 3$. $^{\#}P < 0.05$, $^{\#\#\#}P < 0.001$, vs. control group; $^{*}P < 0.05$, $^{**}P < 0.01$, $^{***}P < 0.001$, vs. CORT group; $^{\&}P < 0.05$, $^{\&\&}P < 0.01$, vs. co-incubation group of purine metabolites and Chaigui granules (CG); ns: no significant difference.

(Fig. 6B). Among them, xanthine (0.005–300 μM) aggravated CORT-induced nerve damage in PC12 cells, whereas adenosine (0.005–5 μM) and inosine (0.005 and 0.05 μM) had opposite effects to xanthine. Interestingly, after co-incubation of CG with xanthine/adenosine/inosine, the neurodamaging effect of xanthine was suppressed, and the neuroprotective effects of adenosine and inosine were promoted (Fig. 6C). Combined with the regulatory effect of CG on purine metabolites in the PFC of CUMS rats, CG exerted antidepressant effects mainly by reducing the level of xanthine and increasing the levels of adenosine and inosine.

3.5. The regulatory effects of CG on P2X7R and A_1R were derived from changes in xanthine and adenosine/inosine levels

Purine metabolites could exert neuromodulatory effects through purinergic receptors. Considering that the trend of xanthine was consistent with P2X7R/A_{2A}R, and the trends of adenosine/inosine were consistent with A_1R in the PFC of CUMS rats, we speculated that xanthine might promote the expression of P2X7R/A_{2A}R, and adenosine/inosine might promote the expression of A_1R. In this section, the effect of xanthine on the expression of

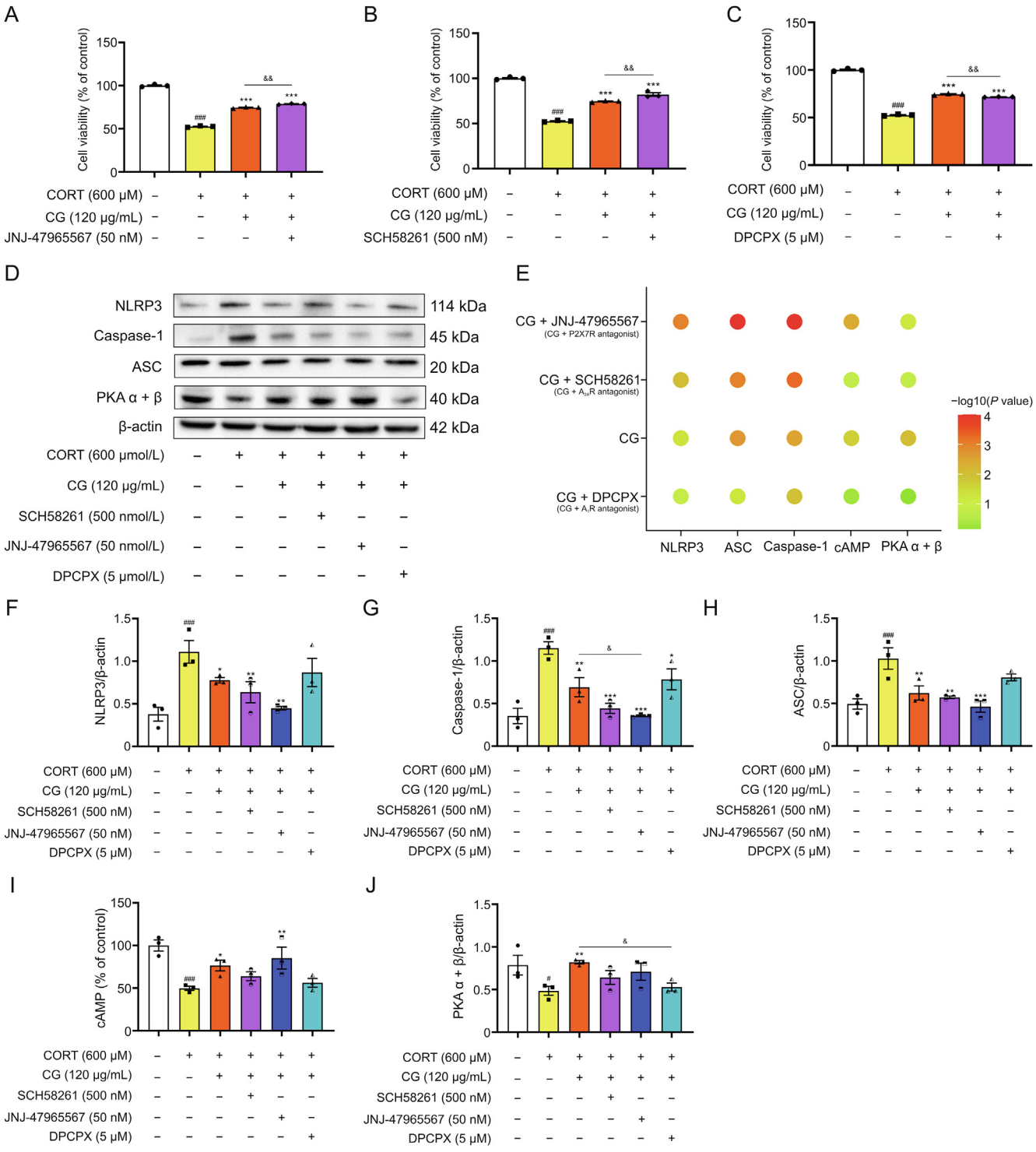

Fig. 8. Effects of P2X7 receptor (P2X7R), A_{2A} receptor (A_{2A}R) and A_1 receptor (A_1R) antagonists on Chaigui granules (CG) neuroprotection and signaling pathways. (A) The neuroprotective effect of CG was promoted by P2X7R antagonist (JNJ-47965567). (B) The neuroprotective effect of CG was promoted by A_{2A}R antagonist (SCH5 8261). (C) The neuroprotective effect of CG was blocked by A_1R antagonist (DPCPX). (D) Western blot of purinergic signaling pathways. (E) Differential effects of P2X7R, A_{2A}R and A_1R antagonists on CG regulation of signaling pathways. The redder the color, the stronger the regulatory effect, while the greener the color, the weaker the regulatory effect. (F) Western blot statistics of Nod-like receptor protein 3 (NLRP3). (G) Western blot statistics of caspase-1. (H) Western blot statistics of apoptosis-associated speck-like protein containing a CARD (ASC). (I) Enzyme-linked immunosorbent assay (ELISA) result for cyclic adenosine monophosphate (cAMP). (J) Western blot statistics of protein kinase A (PKA). Data were presented as mean ± standard error of mean (SEM), $n = 3$. $^{\#}P < 0.05$, $^{\#\#\#}P < 0.001$, vs. control group; $^{*}P < 0.05$, $^{**}P < 0.01$, $^{***}P < 0.001$, vs. CORT group; $^{\&}P < 0.05$, $^{\&\&}P < 0.01$, vs. CG group.

P2X7R/A_{2A}R and the effect of adenosine/inosine on the expression of A_1R were analyzed by immunofluorescence staining. The results showed that the expression of P2X7R/A_{2A}R was significantly increased, whereas the expression of A_1R was significantly decreased in CORT-injured PC12 cells compared to the control group, and the expression changes of these three receptors were reversed after treatment with CG (Figs. 7A–C). After exogenous xanthine supplementation, the expression of P2X7R was further enhanced compared with that in the model group, and this effect was counteracted by CG (Fig. 7D). In contrast, xanthine had no

obvious effect on the expression of $A_{2A}R$ (Fig. 7E). Furthermore, the expression of A_1R was enhanced after exogenous supplementation with adenosine/inosine, and this effect was further promoted by CG (Figs. 7F and G). Combined with animal experiments, the results demonstrated that CG could inhibit the overexpression of P2X7R by reducing xanthine and enhance the expression of A_1R by increasing adenosine and inosine.

Although the cause of $A_{2A}R$ overexpression was not found in this part, it has been shown that $A_{2A}R$ expression is regulated by P2X7R, and $A_{2A}R$ expression can be promoted by P2X7R overexpression [35]. Correspondingly, $A_{2A}R$ overexpression could also promote the expression of P2X7R. Therefore, the increase in $A_{2A}R$ in CUMS rats and CORT-injured PC12 cells may be related to the overexpression of P2X7R.

3.6. The NLRP3 inflammasome pathway was associated with activation of P2X7R/$A_{2A}R$, and the cAMP-PKA pathway was associated with activation of A_1R

To clarify the intrinsic relationship between purinergic receptors and purinergic signaling pathways, the effects of P2X7R, $A_{2A}R$ and A_1R antagonists on the NLRP3 inflammasome pathway and cAMP-PKA pathway were investigated. After dose screening, 50 nM of P2X7R antagonist (JNJ-47965567), 500 nM of $A_{2A}R$ antagonist (SCH58261) and 5 μM of A_1R antagonist (DPCPX) were used in this part (Fig. S7). The results showed that the neuroprotective effect of CG was enhanced by P2X7R/$A_{2A}R$ antagonists (Figs. 8A and B) and counteracted by the A_1R antagonist (Fig. 8C). As further research showed, after P2X7R was antagonized, the suppressive effect of CG on the NLRP3 inflammasome pathway was enhanced (Figs. 8D–H). Interestingly, the $A_{2A}R$ antagonist also appeared to promote the inhibitory effect of CG on the NLRP3 inflammasome pathway (Fig. 8E). Additionally, after A_1R was antagonized, the activation effect of CG on the cAMP-PKA pathway was counteracted (Figs. 8E, I, and J). From the above results, it could be seen that the activation of the A_1R-cAMP-PKA pathway and the inhibition of the P2X7R/$A_{2A}R$-NLRP3 inflammasome pathway were involved in the antidepressant effect of CG.

As important targets of purinergic receptors, both the NLRP3 inflammasome pathway and the cAMP-PKA pathway play essential roles in the regulation of depression. Among them, activation of the cAMP-PKA pathway might exert antidepressant effects by enhancing synaptic plasticity [36], whereas the NLRP3 inflammasome pathway contributes to depression by inducing neuroinflammation [37]. Notably, the cascade of the cAMP-PKA pathway has a potential positive effect on neuroprotection, and broadly alleviates depression-related dysfunction [23]. For example, the cAMP-PKA pathway could increase the level of brain derived neurotrophic factor (BDNF) by acting on the cAMP response element-binding protein (CREB), and alleviate the neuroinflammation caused by the NLRP3 inflammasome. Furthermore, activation of the cAMP-PKA pathway could also improve hypothalamic-pituitary-adrenal (HPA) axis disorder and restore neurotransmitter system. Taken together, the antidepressant

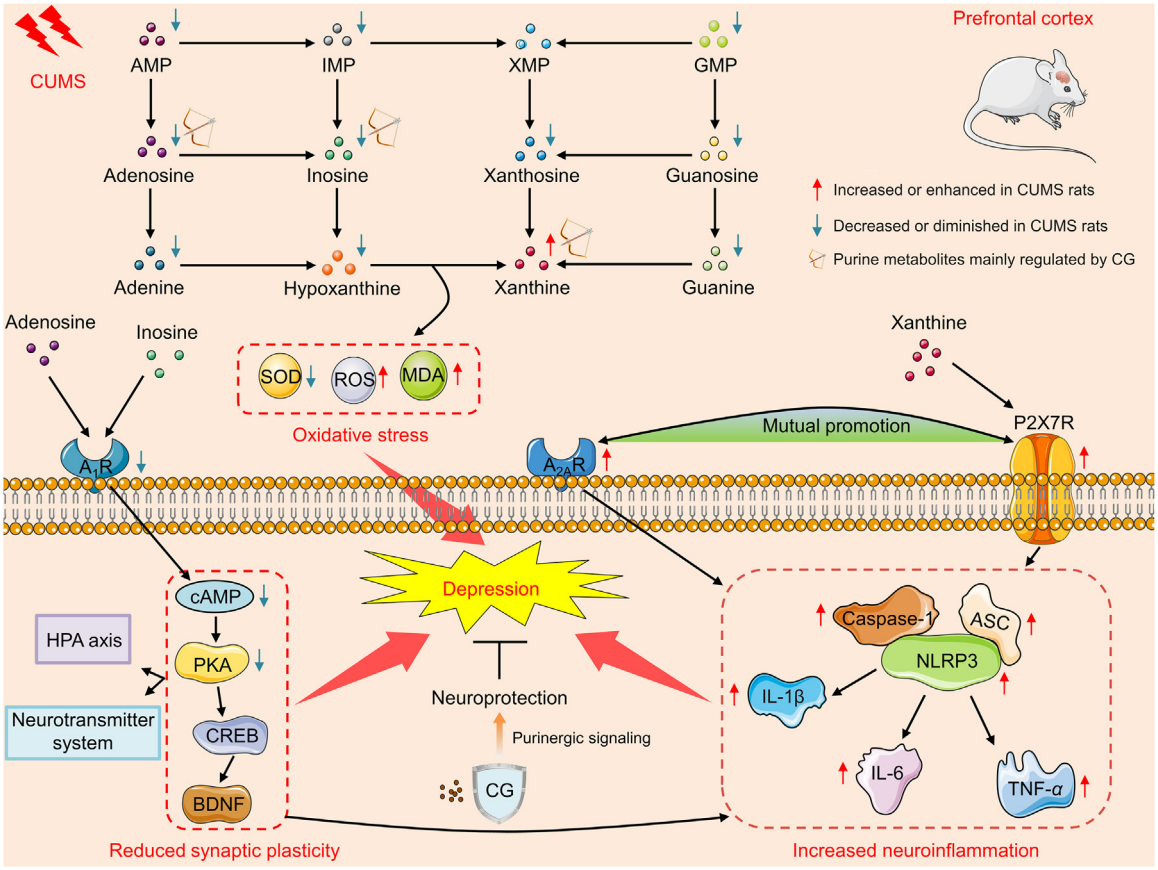

Fig. 9. The antidepressant mechanism of Chaigui granules (CG) by regulating purine metabolism and purinergic signaling. AMP: adenosine-5′-monophosphate; A_1R: A_1 receptor; $A_{2A}R$: A_{2A} receptor; ASC: apoptosis-associated speck-like protein containing a CARD; BDNF: brain derived neurotrophic factor; cAMP: cyclic adenosine monophosphate; CREB: cAMP response element-binding protein; CUMS: chronic unpredictable mild stress; GMP: guanosine-5′-monophosphate; IL-1β: interleukin-1β; IL-6: interleukin-6; IMP: inosine-5′-monophosphate; MDA: malondialdehyde; NLRP3: Nod-like receptor protein 3; PKA: protein kinase A; P2X7R: P2X7 receptor; ROS: reactive oxygen species; SOD: superoxide dismutase; TNF-α: tumor necrosis factor-α; XMP: xanthosine-5′-monophosphate.

mechanism of CG by regulating purine metabolism and purinergic signaling is shown in Fig. 9.

For the first time in this study, the antidepressant mechanism of CG was analyzed from the perspective of the relationship between purine metabolism and purinergic signaling. Among them, three purine metabolites (xanthine, adenosine and inosine) were identified to provide a basis for the screening of potential biomarkers for clinical depression diagnosis. Meanwhile, the antidepressant mechanism of CG elucidated in this study provides a reference for the clinical application guidance of CG and the development of new antidepressant drugs. However, although the present study showed that the antidepressant effect of CG was related to the regulation of purine metabolism and purinergic signaling, some limitations were still observed. The intrinsic link between CG regulation of purine metabolism and purinergic signaling has only been characterized in vitro and needs to be validated in vivo. Furthermore, only the purine metabolites most significantly regulated by CG have been studied in purine metabolism, and the role of other purine metabolites needs to be further investigated. Interestingly, a recent study showed that P2X7R in the brain of CUMS rats was able to regulate depressive-like behavior by affecting immune cells [38], suggesting that the antidepressant mechanism of CG elucidated in this study may also be involved in the regulation of the immune system, and the related biological pathway could be considered for further research.

4. Conclusions

In the present study, UHPLC-MS/MS targeted quantitative analysis and exogenous purine supplementation were integrated to dissect the potential antidepressant mechanism of CG. We found that disordered purine metabolism, abnormal purinergic receptors, and dysregulated purinergic signaling pathways in the PFC of CUMS rats were significantly reversed by CG. Subsequently, the antidepressant effect of CG was determined to be related to the inhibition of the P2X7R/A_{2A}R-NLRP3 inflammasome pathway and the activation of the A_1R-cAMP-PKA pathway. Among them, inhibition of the P2X7R-NLRP3 inflammasome pathway was associated with the reduction in xanthine by CG, and activation of the A_1R-cAMP-PKA pathway was associated with the increase in adenosine and inosine by CG. In summary, CG could promote neuroprotection and ultimately play an antidepressant role by inhibiting the xanthine-P2X7R-NLRP3 inflammasome pathway and activating the adenosine/inosine-A_1R-cAMP-PKA pathway.

CRediT author statement

Jiajun Chen: Methodology, Investigation, Validation, Writing - Original draft preparation, Reviewing and Editing; **Tian Li:** Methodology, Investigation, Writing - Original draft preparation; **Dehua Huang:** Investigation; **Wenxia Gong, Junsheng Tian, Xiaoxia Gao, Xuemei Qin,** and **Guanhua Du:** Supervision; **Yuzhi Zhou:** Funding acquisition, Methodology, Supervision, Writing - Reviewing and Editing.

Declaration of competing interest

The authors declare that there are no conflicts of interest.

Acknowledgments

This work was financially supported by the National Natural Science Foundation of China (Grant Nos.: 82074323 and 81673572), Key Research and Development Program of Shanxi Province (Grant No.: 202102130501010), Innovation Project for Graduate Students in Shanxi Province (Grant No.: 2022Y162), the Major Science and Technology Project for “Significant New Drugs Creation” (Grant No.: 2017ZX09301047), and Research Project Supported by Shanxi Scholarship Council of China (Grant No.: 2020019).

Appendix A. Supplementary data

Supplementary data to this article can be found online at https://doi.org/10.1016/j.jpha.2023.08.008.

References

[1] G.2.D.A.I. Collaborators, Global burden of 369 diseases and injuries in 204 countries and territories, 1990-2019: A systematic analysis for the global burden of disease study 2019, Lancet 396 (2020) 1204–1222.
[2] X. Wang, R. Wang, Q. Ding, et al., Hypochlorous acid-activated multifunctional fluorescence platform for depression therapy and antidepressant efficacy evaluation, Anal. Chem. 94 (2022) 9811–9818.
[3] Y. Zhu, F. Wang, J. Han, et al., Untargeted and targeted mass spectrometry reveal the effects of theanine on the central and peripheral metabolomics of chronic unpredictable mild stress-induced depression in juvenile rats, J. Pharm. Anal. 13 (2023) 73–87.
[4] S. Yao, M. Xu, Y. Wang, et al., Astrocytic lactate dehydrogenase A regulates neuronal excitability and depressive-like behaviors through lactate homeostasis in mice, Nat. Commun. 14 (2023), 729.
[5] K. Fan, Y. Li, H. Wang, et al., Stress-induced metabolic disorder in peripheral $CD4^+$ T cells leads to anxiety-like behavior, Cell 179 (2019) 864–879.e19.
[6] B. Huang, Y. Wu, C. Li, et al., Molecular basis and mechanism of action of *Albizia julibrissin* in depression treatment and clinical application of its formulae, Chin. Herb. Med. 15 (2023) 201–213.
[7] D. Huang, L. Wang, Y. Wu, et al., Metabolomics based on peripheral blood mononuclear cells to dissect the mechanisms of Chaigui Granules for treating depression, ACS Omega 7 (2022) 8466–8482.
[8] J. Tian, P. Qin, T. Xu, et al., Chaigui Granule exerts anti-depressant effects by regulating the synthesis of estradiol and the downstream of CYP19A1-E2-ERKs signaling pathway in CUMS-induced depressed rats, Front. Pharmacol. 13 (2022), 1005438.
[9] G. Burnstock, Purinergic nerves, Pharmacol. Rev. 24 (1972) 509–581.
[10] G. Burnstock, Purinergic signalling and disorders of the central nervous system, Nat. Rev. Drug Discov. 7 (2008) 575–590.
[11] Z. Huang, N. Xie, P. Illes, et al., From purines to purinergic signalling: Molecular functions and human diseases, Signal Transduct. Target. Ther. 6 (2021), 162.
[12] A. Szopa, K. Socała, A. Serefko, et al., Purinergic transmission in depressive disorders, Pharmacol. Ther. 224 (2021), 107821.
[13] X. Zhou, L. Liu, X. Lan, et al., Polyunsaturated fatty acids metabolism, purine metabolism and inosine as potential independent diagnostic biomarkers for major depressive disorder in children and adolescents, Mol. Psychiatry 24 (2019) 1478–1488.
[14] Z. Lu, S. Li, N. Aa, et al., Quantitative analysis of 20 purine and pyrimidine metabolites by HILIC-MS/MS in the serum and hippocampus of depressed mice, J. Pharm. Biomed. Anal. 219 (2022), 114886.
[15] J.M. Deussing, E. Arzt, P2X7 receptor: A potential therapeutic target for depression? Trends Mol. Med. 24 (2018) 736–747.
[16] F. Bartoli, M. Clerici, G. Carrà, Purinergic system and suicidal behavior: Exploring the link between adenosine A2A receptors and depressive/impulsive features, Mol. Psychiatry 25 (2020) 512–513.
[17] V. Lazarevic, Y. Yang, I. Flais, et al., Ketamine decreases neuronally released glutamate via retrograde stimulation of presynaptic adenosine A1 receptors, Mol. Psychiatry 26 (2021) 7425–7435.
[18] J.C. Rech, A. Bhattacharya, M.A. Letavic, et al., The evolution of P2X7 antagonists with a focus on CNS indications, Bioorg. Med. Chem. Lett. 26 (2016) 3838–3845.
[19] M.A. Letavic, B.M. Savall, B.D. Allison, et al., 4-methyl-6,7-dihydro-4H-triazolo[4,5-c]pyridine-based P2X7 receptor antagonists: Optimization of pharmacokinetic properties leading to the identification of a clinical candidate, J. Med. Chem. 60 (2017) 4559–4572.
[20] C.C. Chrovian, A. Soyode-Johnson, A.A. Peterson, et al., A dipolar cycloaddition reaction to access 6-methyl-4,5,6,7-tetrahydro-1H-[1,2,3]triazolo[4,5-c]pyridines enables the discovery synthesis and preclinical profiling of a P2X7 antagonist clinical candidate, J. Med. Chem. 61 (2018) 207–223.
[21] R.O. Godinho, T. Duarte, E.S.A. Pacini, New perspectives in signaling mediated by receptors coupled to stimulatory G protein: The emerging significance of cAMP efflux and extracellular cAMP-adenosine pathway, Front. Pharmacol. 6 (2015), 58.
[22] D.E. Ribeiro, A.L. Roncalho, T. Glaser, et al., P2X7 receptor signaling in stress and depression, Int. J. Mol. Sci. 20 (2019), 2778.
[23] F. Gao, S. Yang, J. Wang, et al., cAMP-PKA cascade: An outdated topic for depression? Biomed. Pharmacother. 150 (2022), 113030.

[24] M. Tang, T. Liu, P. Jiang, et al., The interaction between autophagy and neuroinflammation in major depressive disorder: From pathophysiology to therapeutic implications, Pharmacol. Res. 168 (2021), 105586.
[25] Z. Yan, B. Rein, Mechanisms of synaptic transmission dysregulation in the prefrontal cortex: Pathophysiological implications, Mol. Psychiatry 27 (2022) 445–465.
[26] D.A. Pizzagalli, A.C. Roberts, Correction: Prefrontal cortex and depression, Neuropsychopharmacology 47 (2022), 609.
[27] C. Chen, Q. Yin, J. Tian, et al., Studies on the potential link between antidepressant effect of Xiaoyao San and its pharmacological activity of hepatoprotection based on multi-platform metabolomics, J. Ethnopharmacol. 249 (2020), 112432.
[28] C. Chen, W. Gong, J. Tian, et al., *Radix* Paeoniae Alba attenuates *Radix* Bupleuri-induced hepatotoxicity by modulating gut microbiota to alleviate the inhibition of saikosaponins on glutathione synthetase, J. Pharm. Anal. 13 (2023) 640–659.
[29] X. Zhu, Q. Ma, F. Yang, et al., Xiaoyaosan ameliorates chronic restraint stress-induced depression-like phenotype by suppressing A2AR signaling in the rat *Striatum*, Front. Pharmacol. 13 (2022), 897436.
[30] J. Lu, B. Jia, L. Yang, et al., Ultra-high performance liquid chromatography with ultraviolet and tandem mass spectrometry for simultaneous determination of metabolites in purine pathway of rat plasma, J. Chromatogr. B 1036–1037 (2016) 84–92.
[31] J. Chen, T. Li, X. Qin, et al., Integration of non-targeted metabolomics and targeted quantitative analysis to elucidate the synergistic antidepressant effect of *Bupleurum chinense* DC – *Paeonia lactiflora* pall herb pair by regulating purine metabolism, Front. Pharmacol. 13 (2022), 900459.
[32] M.P. Kaster, A.O. Rosa, M.M. Rosso, et al., Adenosine administration produces an antidepressant-like effect in mice: Evidence for the involvement of A_1 and A_{2A} receptors, Neurosci. Lett. 355 (2004) 21–24.
[33] M.P. Kaster, J. Budni, M. Gazal, et al., The antidepressant-like effect of inosine in the FST is associated with both adenosine A1 and A 2A receptors, Purinergic Signal. 9 (2013) 481–486.
[34] A. Camargo, L.E.B. Bettio, P.B. Rosa, et al., The antidepressant-like effect of guanosine involves the modulation of adenosine A_1 and A_{2A} receptors, Purinergic Signal. 19 (2023) 387–399.
[35] L. Dias, C.R. Lopes, F.Q. Gonçalves, et al., Crosstalk between ATP-P2X7 and adenosine A2A receptors controlling neuroinflammation in rats subject to repeated restraint stress, Front. Cell. Neurosci. 15 (2021), 639322.
[36] W.N. Marsden, Synaptic plasticity in depression: Molecular, cellular and functional correlates, Prog. Neuro-Psychopharmacol. Biol. Psychiatry 43 (2013) 168–184.
[37] J. Rao, Y. Qiao, R. Xie, et al., Fecal microbiota transplantation ameliorates stress-induced depression-like behaviors associated with the inhibition of glial and NLRP3 inflammasome in rat brain, J. Psychiatr. Res. 137 (2021) 147–157.
[38] R. Troubat, S. Leman, K. Pinchaud, et al., Brain immune cells characterization in UCMS exposed P2X7 knock-out mouse, Brain Behav. Immun. 94 (2021) 159–174.